

### Spectroscopic Techniques

Gary E. Martin [1]

Department of Medicinal Chemistry, College of Pharmacy,  
University of Houston, Houston, Texas 77004

Stanford L. Smith and W. John Layton

Department of Chemistry, University of Kentucky,  
Lexington, Kentucky 40506

M. Robert Willcott, III

Department of Chemistry, University of Houston,  
Houston, Texas 77004

Masatomo Iwao and Milton L. Lee

Department of Chemistry, Brigham Young University,  
Provo, Utah 84602

Raymond N. Castle

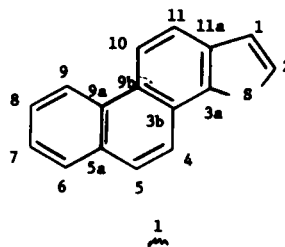
Department of Chemistry, University of South Florida,  
Tampa, Florida 33620

Received March 22, 1983

Two-dimensional nmr spectroscopy, by virtue of its second frequency domain which permits the segregation of spectral information along two frequency axes, considerably simplifies many assignment problems and facilitates others which may be impossible using conventional nmr methodology. A compound which falls into the latter category of assignment problem is phenanthro[1,2-*b*]thiophene. The assignment of the  $^1\text{H}$ - and  $^{13}\text{C}$ -nmr spectra of phenanthro[1,2-*b*]thiophene are, however, reported through the concerted application of two-dimensional nmr techniques. Experiments utilized in making the assignments included: auto-correlated homonuclear (COSY) two-dimensional spectroscopy; heteronuclear two-dimensional J-resolved spectroscopy; proton-carbon chemical shift correlation two-dimensional spectroscopy; and two-dimensional  $^{13}\text{C}$ - $^{13}\text{C}$  double quantum coherence spectroscopy.

*J. Heterocyclic Chem.*, **20**, 1367 (1983).

Polycyclic aromatic compounds (PAC) have long been of interest because of their potential carcinogenicity and mutagenicity [2,3]. More recently, sulfur-containing PACs have garnered additional interest as potential structural components of coal. In particular, polycyclic thiophenes have been isolated from coal fractions by gas chromatography/mass spectrometric techniques [4-7] which has prompted Castle and co-workers to initiate the syntheses of various members of the family of polycyclic thiophenes [8-19]. Due to the growing interest in the examination of fossil fuel samples by cross-polarization magic angle spinning (CPMAS) nmr spectroscopy [20], we were thus interested in attempting the total assignment of the  $^1\text{H}$ - and  $^{13}\text{C}$ -nmr spectra of members of the polycyclic thiophene series to establish a data base for subsequent utilization in the examination of coal samples for the presence of these structural subunits. Thus, we would now like to report the assignment of the  $^1\text{H}$ - and  $^{13}\text{C}$ -nmr spectra of phenanthro[1,2-*b*]thiophene (**1**) [19] through the concerted application of two-dimensional nmr spectroscopic techniques.



Total assignments of the  $^1\text{H}$ - and/or  $^{13}\text{C}$ -nmr spectra of polycyclic aromatic systems represent a substantial challenge to the spectroscopist because of the numbers of resonances in frequently very close proximity. In general, assignments have been based on such considerations as spin-lattice ( $T_1$ ) relaxation times [21-27], deuterium labeling experiments [21,28-34] or the examination of spectra of large numbers of derivatives of a given system [35-39]. The complexity inherent in the spectra of symmetric polycyclic aromatic systems is, in itself, troublesome. In the case of heterocyclic fused ring analogs, the problem is usually fur-

ther complicated since symmetry is destroyed, lending to even further congestion of the spectra. Thus, the assignment of the  $^1\text{H}$ - and  $^{13}\text{C}$ -nmr spectra of polycyclic aromatic thiophenes requires the development of an approach which can be relied upon to lead to unequivocal assignments. For this purpose, we have investigated the concerted utilization of several two-dimensional nmr spectroscopic techniques which has led to the spectral assignment of phenanthro[1,2-*b*]thiophene (**1**).

#### A Strategy for Assigning the Spectra of Phenanthro[1,2-*b*]thiophene.

The conventional  $^1\text{H}$ - and  $^1\text{H}$ -decoupled  $^{13}\text{C}$ -nmr spectra of phenanthro[1,2-*b*]thiophene (**1**) are somewhat bewildering in their complexity. The  $^1\text{H}$ -nmr spectrum (Figure 1)

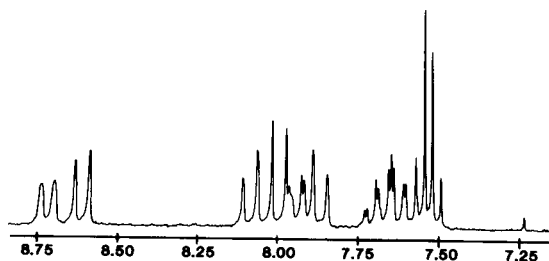


Figure 1. Conventional  $^1\text{H}$ -nmr spectrum of phenanthro[1,2-*b*]thiophene (**1**) in deuteriochloroform at 200 MHz.

is comprised of two AB patterns, an AX pattern and a four proton ABMX pattern which overlap considerably even at 200 MHz, at which the spectrum shown in Figure 1 was taken. The assignment of this spectrum by conventional techniques would, at a minimum, represent a substantial challenge and require the extensive use of iterative nmr fitting programs. Even with such an effort, an unequivocal assignment still might not result. The  $^{13}\text{C}$ -nmr spectrum of **1** is similarly complex (Figure 2), the sixteen carbon resonances clustered in a range of slightly less than 20 ppm with the protonated carbon resonances congested in a range of less than 9 ppm. The development and utilization of chemical shift arguments for the  $^{13}\text{C}$ -nmr spectrum of **1**, although a useful exercise as an initial starting point, would thus also lead to potentially equivocal assignments at best. With the shortcomings obviously inherent in the conventional approaches to the assignment of the spectra of **1**, there is clearly a need for an alternative approach that is capable of yielding unequivocal spectral assignments for these interesting molecules.

Although many potentially useful strategies could be devised for the spectral assignment of **1**, in the ensuing sections of this work we shall describe a strategy which employs the concerted application of several two-dimensional nmr experiments and their execution which leads to an unequivocal assignment of both the  $^1\text{H}$ - and  $^{13}\text{C}$ -nmr spec-

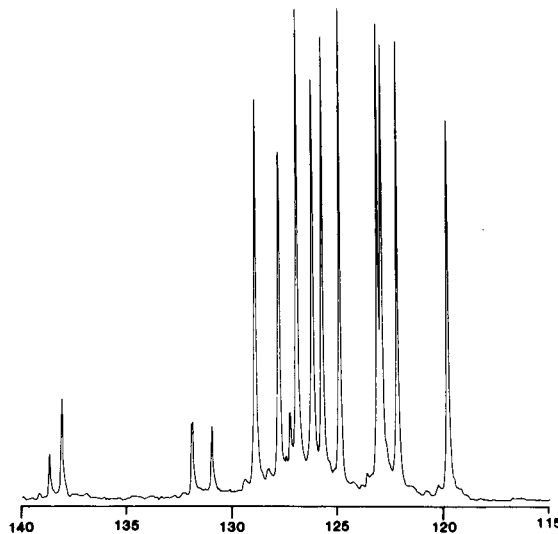


Figure 2.  $^1\text{H}$ -Decoupled  $^{13}\text{C}$ -nmr spectrum of phenanthro[1,2-*b*]thiophene (**1**) in deuteriochloroform at 50 MHz.

tra of **1**. Our assignment strategy begins with an auto-correlated two-dimensional  $^1\text{H}$ -nmr experiment (COSY) [40,41]. Because of the considerable utility of heteronuclear spin-coupling constants and relaxation times in making assignments, the COSY experiment will be followed by the acquisition of a heteronuclear two-dimensional J-resolved (2DJ) spectrum to provide convenient access to the heteronuclear spin-coupling constants and an inversion-recovery experiment to measure the spin-lattice ( $T_1$ ) relaxation times of the protonated carbons. Following the completion of the heteronuclear 2DJ and spin-lattice relaxation time experiments, a two-dimensional proton-carbon chemical shift correlation experiment will next be conducted to complete the carbon assignments or conversely, to complete any necessary proton assignments from a knowledge of carbon chemical shifts. Finally, all of the carbon assignments will, in essence, be verified by the acquisition of a two-dimensional double quantum coherence spectrum although in reality this experiment is intended to complete the assignment of the quaternary carbon resonances which have not been otherwise dealt with.

#### Fundamental Considerations and Conventions of Two-Dimensional NMR Spectroscopy.

Two-dimensional Fourier transform (2DFT) nmr spectroscopy represents far more than a simple alternative means of data display. These techniques make use of rather formidable data matrices acquired in terms of two discrete time variables,  $t_1$  and  $t_2$  [42], which are then subjected to double Fourier transformation [40,43] to provide intensity information which is a function of two frequencies,  $F_1$  and  $F_2$ . Since these techniques are relatively new,

it is worth investing some time in addressing the implementation and processing of two-dimensional nmr spectra which will considerably augment the understandability of the two-dimensional experiments which are subsequently employed in the assignment of the spectra of **1**.

Numerous considerations are inherent in an understanding of two-dimensional nmr spectroscopy, perhaps one of the most fundamental is that of the nomenclature used to describe the experiments and the data processing. As mentioned above, resonances in two-dimensional nmr spectra are initially defined in terms of two simultaneously running time variables which are converted to the frequency domain, from a transformation with respect to each time variable. By convention, the initial time domain data set is denoted  $S(t_1, t_2)$ . Since thinking in terms of two simultaneously running time variables is a non-trivial undertaking, let us first consider the time domain information contained in a conventional nmr experiment.

Conventional Fourier transform (FT) nmr experiments, in the simplest sense, consist of a preparation period (during which excitation occurs) and an observation or acquisition period during which data sampling in the time domain occurs. Data acquired during the latter phase of the experiment (in the time domain) is denoted  $S(t_2)$ . Fourier transformation of this set of time domain data points then provides a spectrum in the more familiar and interpretable frequency domain which may be denoted  $S(F_2)$ .

Introducing a second time variable into the framework of a conventional nmr experiment complicates matters somewhat, and we find it convenient to introduce this facet of the experiment by a reconsideration of the salient features of the somewhat more familiar spin-lattice relaxation experiments, for example the inversion-recovery experiment [44,45]. Since the spin-lattice relaxation time represents a recovery of magnetization along the  $z'$ -axis, which we have no means of measuring directly, we utilize an additional period in the experiment during which relaxation is allowed to occur for some period of time followed by a pulse designed to sample the evolved magnetization [46]. By conducting a series of such experiments, the evolved magnetization is sampled as a function of spin-lattice relaxation which has transpired during the interval between the two pulses. By evaluating resonance intensities as a function of evolution time, it is then possible to mathematically compute the relaxation time. In the time domain, we may denote a relaxation data set of the type just described by  $S(t_1, t_2)$ , where the time variable  $t_2$  is identical to that of a conventional nmr experiment and the interval  $t_1$  is the evolution period between pulses. Since the desired form of the data from this experiment is frequency information as a function of the evolution duration, we may then perform a single Fourier transform to give an  $S(t_1, F_2)$  data set which when stack plotted

resembles a three dimensional surface.

Two-dimensional nmr experiments are but an extension of the relaxation data set just described. They differ in terms of the number of  $t_1$  intervals employed and the way in which the interval itself is incremented. In this fashion, information contained in the  $t_1$  domain is amenable to the performance of a second Fourier transform such that responses in the spectrum which is finally plotted are a function of two frequencies,  $F_1$  and  $F_2$ . By careful control of the events which transpire during the evolution period, different information can be built into the two frequency domains which are ultimately obtained. The reader interested in the design of two-dimensional nmr experiments is referred to the 1979 report of Ernst and co-workers [46] which describes a variety of possible experiments.

#### Cross-Correlated *vs.* Auto-Correlated Two-Dimensional NMR Experiments.

In the broadest sense, two-dimensional nmr experiments may be subdivided into two general categories; cross-correlated and auto-correlated. As the name implies, cross-correlated 2D experiments correlate different features which may or may not be common to more conventional experiments. For example, useful forms of cross-correlated data include correlation of  $^{13}\text{C}$ -nmr chemical shift information with the heteronuclear  $^1\text{H}$ - $^{13}\text{C}$  spin-coupling constants, correlation of  $^{13}\text{C}$ -chemical shifts with proton chemical shifts or potentially any number of other similar pairs. Auto-correlated 2D spectra, in contrast, refer to those experiments in which the spectrum is in some way correlated with itself. Examples of this type of experiment include auto-correlation by homonuclear spin-coupling (COSY), auto-correlation by homonuclear NOE or other variants. Both types of two-dimensional nmr experiments will be employed in the assignment of the spectra of phenanthro[1,2-*b*]thiophene.

#### Two-Dimensional NMR Data Processing.

The transformation of a two-dimensional data set from the time domain,  $S(t_1, t_2)$ , to the frequency domain,  $S(F_1, F_2)$ , is a relatively complex operation. In principle, the operation could be performed in place if sufficient computer memory were available which would make the entire operation transparent to the user. There are, however, advantages to understanding the processing sequence although it is probable that developments in computer technology will eventually bring along a level of sophistication which will allow the disinterested user to divest himself from the processing, treating it as a black box in a manner analogous to the way in which many users consider the Fourier transformation process.

Once the  $S(t_1, t_2)$  data set has been acquired (individual protocols for the specific experiments utilized in the assignment of the spectra of phenanthro[1,2-*b*]thiophene are

discussed below) we may embark on its processing. The first step in processing a two-dimensional nmr data set is Fourier transformation with respect to  $t_2$ , which converts our initial data set to  $S(t_1, F_2)$ . This operation provides us with frequency information as a function of time. Generally, the frequencies of interest will be modulated in some way as a function of time and thus are amenable to the second Fourier transformation. An example of an amplitude modulation of a carbon resonance is shown in Figure 3.

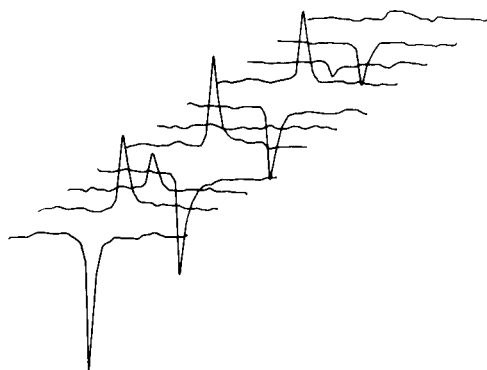


Figure 3. Amplitude modulation of a  $^{13}\text{C}$ -resonance induced by heteronuclear spin-coupling as a function of the duration of the evolution period.

Since at this point in the data processing the time dependent information cannot be loaded into memory, it is next necessary to convert the  $S(t_1, F_2)$  matrix to a form which can be handled in the laboratory computer. The process to accomplish this is known as transposition and is shown schematically in Figure 4. Quite literally, the transposition

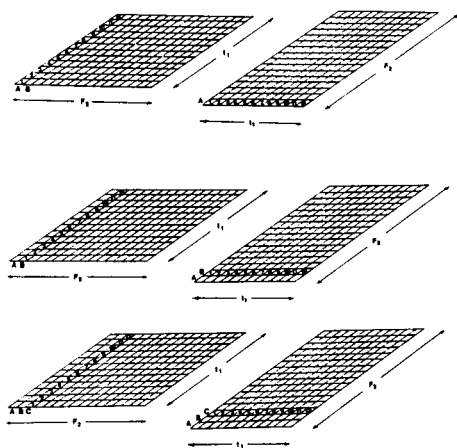


Figure 4. Schematic representation of the transposition process. Points  $A_1$ - $A_{12}$  which are contained in successive  $S(t_1, F_2)$  files become the first data file of the newly formed  $S(F_2, t_1)$  data matrix. Treatment of successive points, B, C,

... *etc.* completes the generation of the  $S(F_2, t_1)$  data matrix which, in effect, gives a set of files which are amenable to Fourier transformation and which further show the time dependent behavior of resonances as a function of frequency.

process involves an exchange of the rows and columns in the  $S(t_1, F_2)$  matrix to give files which contain time domain information as a function of altered frequency, these labeled  $S(F_2, t_1)$ . Practically, transposition produces a second set of data files which strongly resemble the initial free induction decays (FID's). The appearance of these  $S(F_2, t_1)$  files is illustrated in Figure 5 which contains the interferograms [47] obtained by transposition in the vicinity of the amplitude modulated resonance shown in Figure 3. Fourier transformation of the interferograms generated by transposition then provides responses which are a function of two frequencies,  $S(F_2, F_1)$ . In the case of the interferograms shown in Figure 5, their Fourier transformed result is a doublet of doublets which is shown in Figure 6 as a white-washed stack plot.

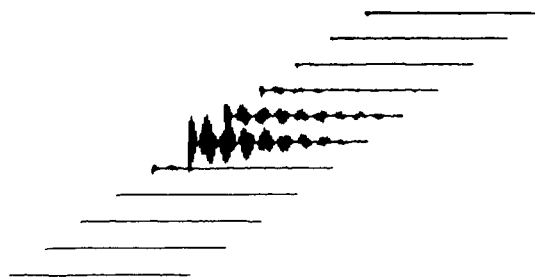


Figure 5.  $S(F_2, t_1)$  interferograms obtained by the transposition of files surrounding the amplitude modulated resonance shown in the  $S(t_1, F_2)$  files illustrated in Figure 3.

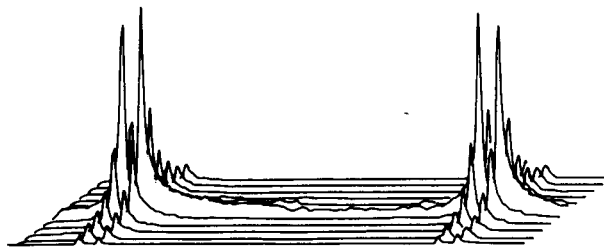


Figure 6.  $S(F_2, F_1)$  result obtained by the Fourier transformation with respect to  $t_1$  of the interferograms shown in Figure 5.

Having processed two-dimensional nmr data to the stage of the  $S(F_2, F_1)$  data matrix, there are a number of possibilities depending upon the specific requirements of the user and the particular experiment being performed.

Some of the alternatives available are combined with the data processing sequence shown as a flow chart in Figure 7.

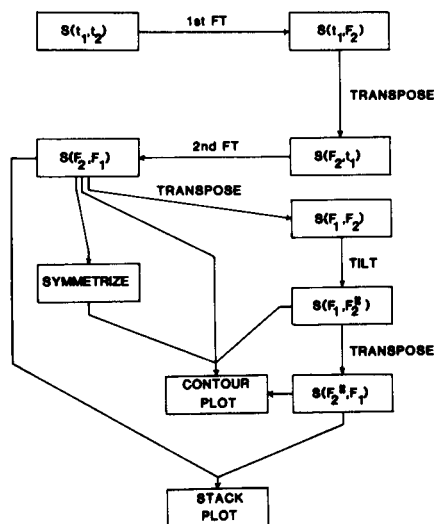


Figure 7. Flow chart illustrating the steps in the processing of two-dimensional nmr spectral data, the steps to be utilized depending upon the experiment whose data is being processed. Not all steps will be utilized in the processing of the data from any one experiment.

#### White-Washed Stack Plots vs. Contour Plots.

Several alternatives are available for data display in two-dimensional nmr spectroscopy. First, we may plot a stack plot analogous to those routinely employed for relaxation experiments. However since two-dimensional nmr spectra may frequently contain hundreds of separate traces, it is easy to understand how information would become obscured by overlap. This obstacle is, in part, circumvented by the "white-wash" routine in which the pen is lifted by the computer whenever a given point in a preceding trace has a higher intensity than that presently being plotted. Although this improves matters somewhat, resonances can still be obscured by other resonances in the stack plot, which has necessitated the development of the contour plot to provide unrestricted representation of two-dimensional data matrices. Basically, contour plots are exactly analogous to the familiar topographic maps employed to depict the earth's surface. The plot is drawn as a series of contours and provides a view of the two-dimensional data matrix which would be obtained if one were to look down on a stack plot from directly above it. Because of their considerably greater ease of interpretation, we shall exclusively employ contour plots to present the two-dimensional nmr data for phenanthro[1,2-*b*]thiophene.

Calculated  $^{13}\text{C}$ -NMR Chemical Shifts of Phenanthro[1,2-*b*]thiophene (**1**).

Although calculated  $^{13}\text{C}$ -nmr chemical shifts may be expected to have only limited utility in polycyclic systems such as **1**, they are useful nevertheless for making preliminary assignments and for drawing comparisons to related systems once the spectra of the first member in the series has been unequivocally assigned. In the case of phenanthro[1,2-*b*]thiophene (**1**), the calculation of  $^{13}\text{C}$ -nmr chemical shifts may be begun by first deriving shift additivities from the assigned  $^{13}\text{C}$ -nmr spectrum of benzothiophene [48] for the fusion of the thiophene ring onto benzene. Given these additivities, the assigned  $^{13}\text{C}$ -nmr chemical shifts of phenanthrene [39] may then be incremented or decremented accordingly for the [1,2-*b*] fusion of the thiophene ring onto the phenanthrene nucleus. The results obtained in this manner are shown in Figure 8. It should also be noted that this method of calculating the

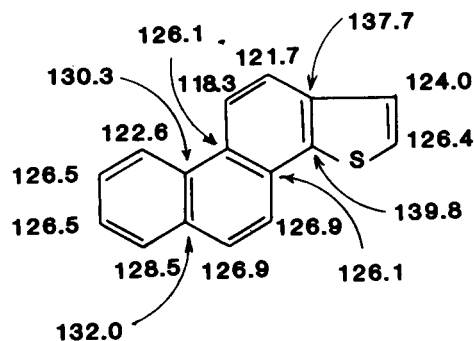


Figure 8. Calculated  $^{13}\text{C}$ -nmr chemical shifts of phenanthro[1,2-*b*]thiophene (**1**) obtained by incrementing the assigned  $^{13}\text{C}$ -nmr chemical shifts of phenanthrene for the [1,2-*b*] fusion of the thiophene ring onto the phenanthrene nucleus.

chemical shifts of **1** ignores potential effects due to the thiophene fusion on all but the directly involved ring of the phenanthrene system. As a consequence of this flaw in the calculation process, various pairs of carbons of **1** are predicted to have identical chemical shifts. In contrast, the  $^1\text{H}$ -decoupled  $^{13}\text{C}$ -nmr spectrum of **1** clearly demonstrates the presence of sixteen resonances (Figure 2), evidencing the shortcoming in the calculation method. Thus, calculated chemical shifts of phenanthrothiophenes and other polynuclear thiophenes must clearly be employed with considerable caution.

#### $^1\text{H}$ - and $^{13}\text{C}$ -NMR Spectral Assignment of Phenanthro[1,2-*b*]thiophene (**1**).

Having laid the groundwork for the spectral assignment of phenanthro[1,2-*b*]thiophene (**1**) with the calculation of the  $^{13}\text{C}$ -nmr chemical shifts using conventional methods,

M. Iwao, M. L. Lee and R. N. Castle

we may next turn our attention to specific aspects of the assignment. The carbon skeleton of **1**, which is similar to that of a steroid, would also be expected to undergo anisotropic reorientation. More specifically, it would be expected that an axis of anisotropic reorientation should pass through the molecule between C1 and C2 on the thiophene end of the molecule and between C7 and C8 on the opposite end of the molecule. To probe this behavior, which can be a useful assignment criterion for heteroaromatic systems [49-53], it is necessary to first collect spin-lattice ( $T_1$ ) relaxation data for the molecule. From an inversion-recovery [44,45] experiment, the data obtained was reduced using the Three-Parameter Fitting program of Kowalewski and co-workers [54] to afford the relaxation times contained in Table I. From these data, it should be

Table I

Protonated carbon spin-lattice ( $T_1$ ) relaxation times for phenanthro[1,2-*b*]thiophene (**1**) in deuteriochloroform at 25.2 MHz. Relaxation data was obtained using the inversion-recovery experiment, the resultant data reduced using the Three-Parameter Fitting Program [54].

Chemical Shift ( $\delta$ )	Relaxation Time (sec)
128.74	$3.3 \pm 0.06$
127.63	$3.3 \pm 0.04$
126.79	$3.6 \pm 0.02$
126.04	$2.4 \pm 0.04$
125.59	$2.5 \pm 0.03$
124.75	$3.1 \pm 0.03$
122.94	$3.4 \pm 0.04$
122.76	$3.2 \pm 0.06$
122.02	$3.5 \pm 0.05$
119.67	$3.3 \pm 0.07$

noted that two resonances, those at  $\delta = 126.04$  and 125.59, exhibit relaxation times which are significantly shorter than those of the remaining carbons, this observation supporting the contention that **1** is indeed subject to anisotropic reorientation. In addition to support for anisotropic reorientation of **1**, the shorter relaxation times of

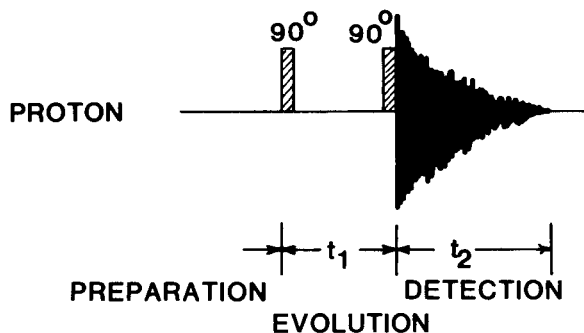


Figure 9. Pulse sequence schematic for the auto-correlated (COSY)  $^1\text{H}$ -nmr experiment. Phase cycling of the second  $90^\circ$  pulse produces the equivalent of quadrature detection in the second dimension and further aids in the elimination of unwanted peaks in the spectrum which are due to longitudinal relaxation occurring during the evolution period.

the two resonances, at a minimum, provide a basis for assigning two additional resonances. Further, since the C2 resonance is expected to be assignable on the basis of its one bond coupling constant [55], if the axis of anisotropic reorientation passes through C1 this will provide additional assignment data.

#### Auto-Correlated Two-Dimensional Homonuclear NMR (COSY).

The auto-correlated two-dimensional homonuclear nmr experiment (COSY or HOMCOR in the Varian XL-200 operating software) utilizes the pulse sequence originally proposed for 2D-nmr spectroscopy by Jeener [40,41,57]. The pulse sequence, which is shown schematically in Figure 9, employs a  $90^\circ$  pulse to excite the spin systems followed by an evolution period ( $t_1$ ) which serves to label the spins with their characteristic precession frequencies followed by a  $90^\circ$  observation pulse which is phase cycled to eliminate axial peaks and artifacts [58,59]. The results obtained from the execution of this experiment on **1** are shown in Figure 10 as a six level contour plot of the entire

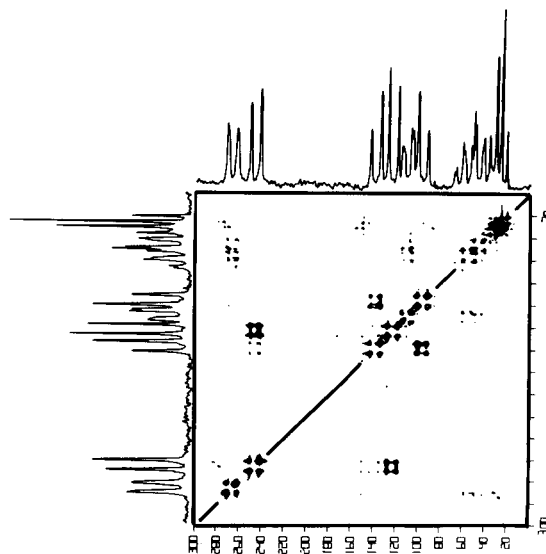


Figure 10. Contour plot of the auto-correlated  $^1\text{H}$ -nmr spectrum of phenanthro[1,2-*b*]thiophene (**1**). The spectrum is correlated with itself as shown by the two projections through  $F_1$  and  $F_2$ , each of which reproduces the conventional  $^1\text{H}$ -nmr spectrum as shown in Figure 1. The spectrum runs along the diagonal while coupled spins give rise to the off-diagonal signals as described in the text, these signals correlating coupled spins.

spectrum. It will be noted that both axes of this experiment,  $F_1$  and  $F_2$ , correspond to proton chemical shift as was discussed above when auto- and cross-correlated 2D experiments were differentiated. From this it follows that

the intense contours appearing along the diagonal (lower left to upper right) correspond to the conventional one-dimensional spectrum shown in Figure 1. In addition to the peaks along the diagonal, there are also off-diagonal peaks which correlate spin-coupled resonances. It is this latter type of peak which is of interest in this experiment, and since off-diagonal peaks establish spin-coupling networks for even closely spaced resonances, which could by no means be decoupled in a conventional fashion, the technique has tremendous potential utility.

Having briefly described the basic types of information contained in the auto-correlated homonuclear experiment, we may now begin to make assignments within the <sup>1</sup>H-nmr spectrum of **1**. While there are numerous ways in which to approach this assignment, it is perhaps most convenient to begin making assignments from the doublet resonating furthest downfield in the conventional proton nmr spectrum at  $\delta = 8.72$ . Since the protons located at the 9- and 10-positions of **1** must clearly account for the resonances further downfield [60], we may establish the identity of the doublet at  $\delta = 8.72$  by elucidating its spin-coupling network from the auto-correlated spectrum. Thus, since the doublet at  $\delta = 8.72$  exhibits off-diagonal peaks which correlate it with the resonances observed at  $\delta = 7.62/7.66$ , these further correlated to yet another proton resonance, then the doublet in question must be part of the four spin ABMX system which allows the assignment of the downfield most doublet at H9 (Figure 11). The assignment of

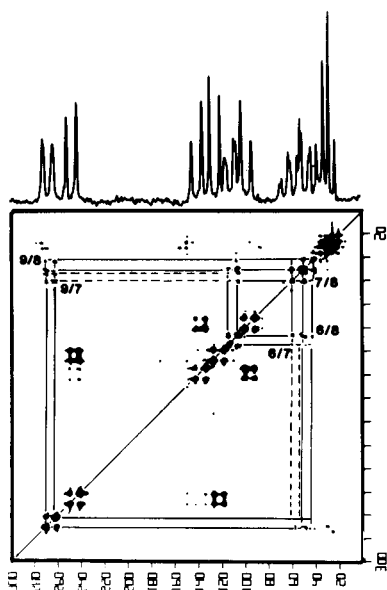


Figure 11. Contour plot of the auto-correlated <sup>1</sup>H-nmr spectrum of phenanthro[1,2-*b*]thiophene (**1**) showing the ABMX spin-coupling network comprised by the H6, H7, H8 and H9 spins. For an enlargement of the detail of the diagonal and off-diagonal signals for the H6, H7 and H8 resonances, see also Figure 14.

the H9 resonance also then allows the assignment of the doublet at  $\delta = 8.61$ , which is part of a two spin AX system, to H10. Through off-diagonal peaks (Figure 12) the doublet at  $\delta = 8.61$  is correlated to the doublet at  $\delta = 8.00$  which is thus assigned as the H11 resonance. In addition

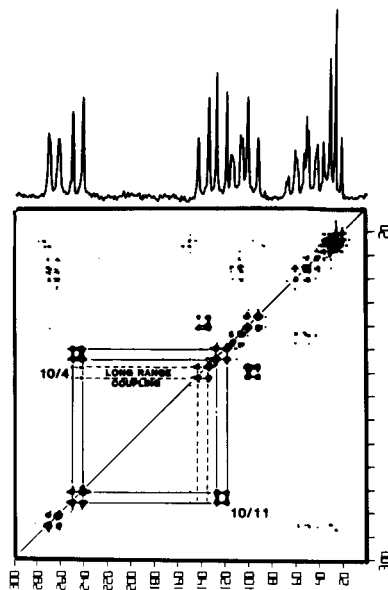


Figure 12. Contour plot of the auto-correlated <sup>1</sup>H-nmr spectrum of phenanthro[1,2-*b*]thiophene (**1**) showing the AX spin-coupling network comprised by the H10 and H11 spins. Also note the long range coupling between H10 and H4 (denoted by dashed lines) which is detectable only by decoupling in the conventional spectrum.

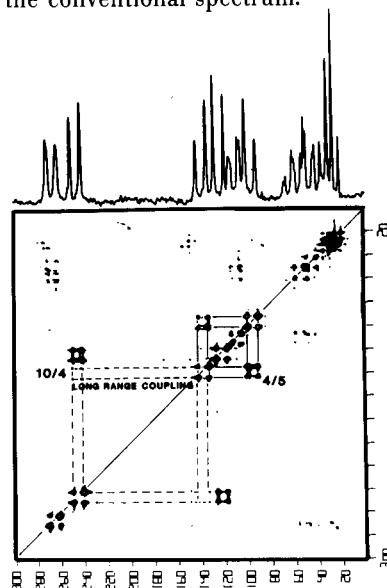


Figure 13. Contour plot of the auto-correlated <sup>1</sup>H-nmr spectrum of phenanthro[1,2-*b*]thiophene (**1**) showing the AB spin-coupling network comprised of the H4 and H5 spins. Also note the long range coupling between H4 and H10 (dashed lines).

to the principle coupling to the H11 resonance, the H10 resonance also exhibits a small long range coupling (five bonds) to a doublet at  $\delta = 8.09$  which forms a part of another AB spin system (Figure 13). It should be noted that the small coupling brought out by the auto-correlated spectrum is by no means readily visible in the conventional  $^1\text{H}$ -nmr spectrum. However, by conventional decoupling of the doublet at  $\delta = 8.61$ , there is a slight sharpening of the doublet at  $\delta = 8.09$  thus providing a secondary proof for the existence of the spin-coupling network. Although the doublet observed at  $\delta = 8.09$  which is long range coupled to the H10 resonance could presumably be either the H1 or the H4 resonance, we will see below that this resonance is correctly assigned to H4, the assignment confirmed by the heteronuclear 2DJ and proton-carbon chemical shift correlation (HETCOR) experiments. The remaining AB spin system, which appeared as a substantially non-first order pattern in the conventional spectrum ( $\delta = 7.55$  and  $7.51$ ) was ultimately assigned to the H2/H1 protons (respectively) of the thiophene portion of the molecule (Figure 14).

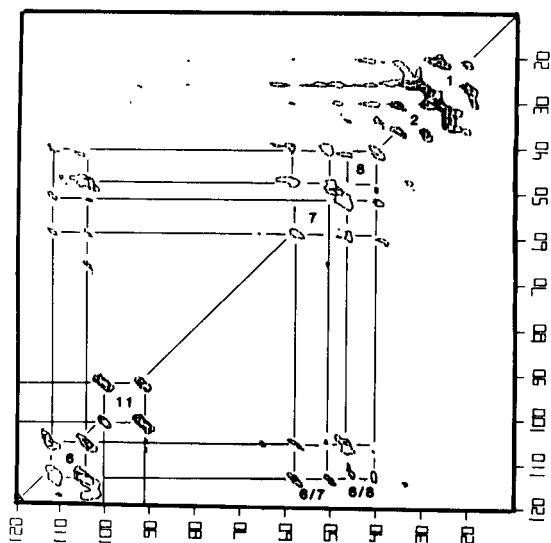


Figure 14. Contour plot of the auto-correlated  $^1\text{H}$ -nmr spectrum of phenanthro[1,2-*b*]thiophene (**1**) showing, on an enlarged scale, the strongly coupled AB spin system consisting of the H1 and H2 resonances. Detail of the diagonal and off-diagonal resonances for H6, H7 and H8 are also shown.

Through the utilization of auto-correlated homonuclear nmr experiments (COSY or HOMCOR), it is clear that spin-coupling networks may be conveniently elucidated. In those cases where bases exist for establishing assignments within the spin-coupling networks, this technique clearly simplifies the assignment process and obviates the tedious computer simulation of spin systems. Finally, the utility of

the auto-correlated  $^1\text{H}$ -nmr experiment in highlighting small, long-range couplings which could easily be missed in conventional spectra is also clear.

#### Heteronuclear Two-Dimensional J-Resolved NMR Spectra.

Following Jeener's 1971 suggestion of the two-dimensional nmr experiment [56], several years elapsed before the first execution of any two-dimensional experiment. The first demonstration of the viability of two-dimensional nmr spectroscopy was the simple (in the context of contemporary two-dimensional nmr experiments presently being employed) heteronuclear experiment of Müller, Kumar and Ernst [61] which resolved the  $^1\text{H}$ - $^{13}\text{C}$  spin-coupled spectrum of *n*-hexane. Since that initial report, a number of other heteronuclear 2DJ-resolved experiments have been described, including the amplitude modulated experiment [62] which was employed in the extraction of the heteronuclear spin-couplings of **1**. While there are minor differences between the various heteronuclear 2DJ nmr experiments [43,61-64], all derive their utility from their ability to sort chemical shifts along the  $F_2$  axis and to display spin-coupling information along the orthogonal  $F_1$  axis. This feature allows the investigation of heteronuclear spin-coupling constants with the same facility of the selective excitation experiments which preceded it [49,66-71]. Since it is the overlap of spin-multiplets which eventually makes the extraction of heteronuclear spin-coupling information from the proton-coupled  $^{13}\text{C}$ -nmr spectra of large molecules intractable, the utility of the heteronuclear 2DJ experiment is quite clear.

Table II

Proton chemical shifts and coupling constants for phenanthro[1,2-*b*]thiophene (**1**) in deuteriochloroform relative to internal TMS.

Position	Chemical Shift ( $\delta$ )	Coupling (Hz)
1	7.51	$J_{1,2} = 5.37$
2	7.55	
4	8.09	$J_{4,5} = 8.8$
5	7.87	
6	7.94	$J_{6,7} = 7.6$
7	7.66	$J_{7,8} = 6.5$
8	7.62	$J_{8,9} = 7.8$
9	8.72	
10	8.61	$J_{10,11} = 8.8$
11	8.00	

The pulse sequence utilized in the examination of the heteronuclear spin-coupling constants of **1** is shown in Figure 15. Gating the decoupler off during the second half of the evolution period in this experiment and then back on during the acquisition period leads to the accumulation of an FID in which individual decoupled  $^{13}\text{C}$ -resonances are amplitude modulated as a function of the duration of the evolution period. In this fashion, the second Fourier transformation which is ultimately performed on this data



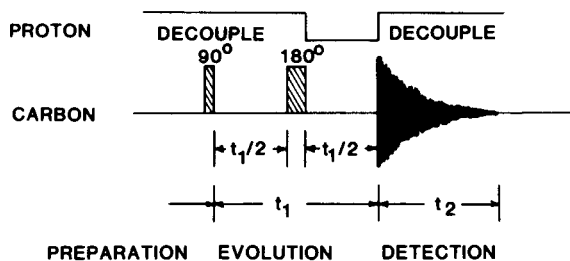


Figure 15. Pulse sequence schematic for the cross-correlated heteronuclear two-dimensional NMR experiment. Heteronuclear spin-couplings, in this experiment, produce an amplitude modulation of the individual carbon resonances as illustrated by the traces shown in Figure 3.

set produces a spin-coupled sub-spectrum for the individual resonances, spin-coupling information displayed orthogonally to the chemical shift or  $F_2$  axis. Equipped with a knowledge of the spin-coupling constant behavior likely to arise from phenanthro[1,2-*b*]thiophene (**1**), we may begin to utilize the spin-coupling information derived from the heteronuclear 2DJ experiment for assignment purposes.

Assignments based on heteronuclear spin-coupling constants, both one bond and longer range, have been extensively utilized in the assignment of the <sup>13</sup>C-NMR spectra of a number of heterocyclic systems [49,68-75]. In the case of **1**, however, only a single carbon assignment can be made through the heteronuclear 2DJ experiment although, as we shall see below, this assignment is crucial for completing the proton assignment for H2 and thus that of the C1 and C2 resonances. Specifically, with the exception of the C2 resonance of **1**, all of the remaining protonated carbons were expected to exhibit spin-coupling constants in the range of 160-165 Hz [39]. The C2 resonance, in contrast, was expected to exhibit a one-bond spin-coupling constant in the range 180-185 Hz which is typical for this position of five-membered heterocyclic systems [55]. Thus, the carbon resonance observed at  $\delta = 125.59$  was assigned to C2 on the basis of the 184.4 Hz one-bond coupling which it exhibited. It should also be noted that this resonance was also one of the two resonances observed to possess a significantly shorter relaxation time (Table I), thus providing a preliminary identification of the other carbon with a short relaxation time as either C7 or C8. The remaining one bond coupling constants, as expected were unremarkable.

Although a seemingly large amount of work was entailed in the assignment of the C2 resonance through the heteronuclear 2DJ experiment, it should be kept in mind that there is no simple, alternative means to employ in making this assignment. Furthermore, since all spin-coupling

constant information is obtained simultaneously, it has an advantage over randomly performing selective excitations until the proper resonance is uncovered. Finally, since resolution in the second dimension of this and all spin-echo based two-dimensional NMR experiments is governed by the natural line width ( $T_2$ ) [43,63,76-78], the effects of inhomogeneity which frequently prevent the resolution of small, long-range coupling constants is circumvented hence providing information which is potentially useful for assignment purposes in other systems although it was of relatively little utility in the case at hand.

#### Proton-Carbon Chemical Shift Correlation Spectroscopy.

Although the auto-correlated homonuclear and the J-resolved heteronuclear two-dimensional experiments described above provided significant pieces of information toward the total spectral assignment of phenanthro[1,2-*b*]thiophene, the majority of the protonated carbon resonances remain to be assigned. To accomplish the assignment of the protonated carbon resonances, a two-dimensional proton-carbon chemical shift correlation (HETCOR in the Varian XL-200 operating software) experiment was performed. While similar to the J-resolved heteronuclear two-dimensional experiment just described, in at least some senses, there is a considerable difference in the relative complexity of the pulse sequence used to drive the experiment. Unlike the J-resolved experiment, the proton decoupler is not merely gated on and off. Rather, the proton decoupler is also employed to apply phase coherent 90° pulses to the proton spin system during the course of the experiment, as described below.

Table III

One-bond heteronuclear spin-coupling constants observed for phenanthro[1,2-*b*]thiophene (**1**) in deuteriochloroform.

Chemical Shift ( $\delta$ )	$J_{CH}$
128.74	157.6
127.63	160.6
126.79	159.4
126.04	161.0
125.59	184.4
124.75	168.8
122.94	154.9
122.76	159.6
122.02	162.2
119.67	158.8

The basic principles of the proton-carbon chemical shift correlation was described by Maudsley and Ernst [79] and relies on the indirect detection of proton chemical shift information through the <sup>13</sup>C-nuclide. Although there have been several additional reports in the literature which have described various refinements of the original experiment [80-87], there have been rather few practical applications of the experiment [84,88,89] of which none of these examples are heteroaromatic systems.

M. Iwao, M. L. Lee and R. N. Castle

Modulation of carbon resonances to reflect proton chemical shifts (indirect proton observation) is induced by using the pulse sequence shown in Figure 16. The experiment begins with the application of a  $90^\circ$  proton pulse applied from the decoupler coils of the spectrometer, the

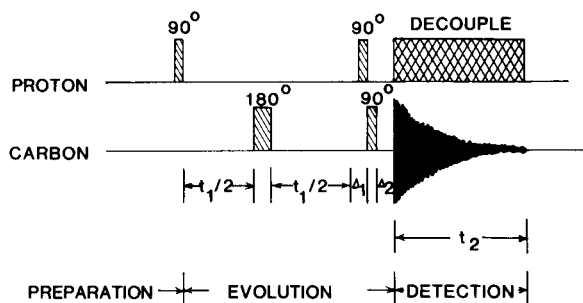


Figure 16. Pulse sequence schematic for the proton-carbon chemical shift correlation two-dimensional nmr experiment. Proton pulses are applied *via* the decoupler coils. The function of the individual pulses and delays are described in detail in the text.

completion of which begins the evolution period. Midway through the evolution period, a  $180^\circ$  carbon pulse is applied which serves to invert the carbon spin labels. At the end of the evolution period, a second  $90^\circ$  proton pulse is applied from the decoupler coils followed by the application of a  $90^\circ$  carbon observation pulse, these flanked by two fixed delays. Following the completion of the second fixed delay,  $\Delta_2$ , the proton decoupler is gated back on and the carbon free induction decay (FID) is collected. Variation of the duration of the evolution period thus leads to the construction of a data matrix of the form  $S(t_1, t_2)$  as in the previous two-dimensional experiments. Fourier transformation with respect to  $t_2$  then leads to a set of spectra,  $S(t_1, F_2)$ , in which the individual carbon resonances are amplitude modulated as a function of the proton resonance frequencies. Upon completion of the data processing, carbon chemical shifts (decoupled) are displayed along the  $F_2$  axis while proton chemical shifts (with multiplet structure intact) are displayed along the  $F_1$  axis. Projection of the data matrix through the  $F_2$  dimension recovers the proton-decoupled  $^{13}\text{C}$ -nmr spectrum while projection through the  $F_1$  dimension recovers the conventional proton spectrum, as shown by the projections flanking Figure 17. Consequently, points of intensity in the contour plot shown in Figure 17 directly correlate the proton spin-multiplets with the carbon to which the proton in question is directly attached.

Since the proton-carbon chemical shift correlation experiment is considerably more complex than the other two-dimensional experiments utilized above, a somewhat more

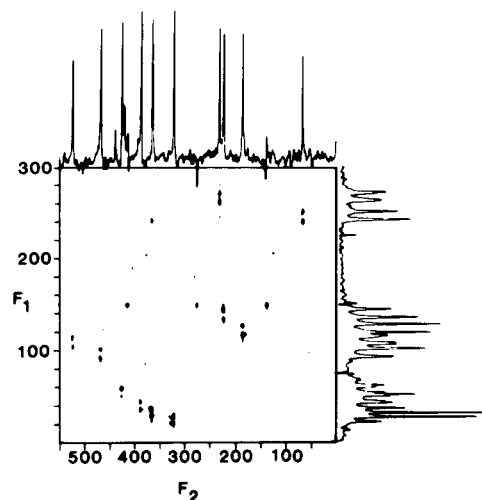


Figure 17. Contour plot of the two-dimensional proton-carbon chemical shift correlation experiment. Projection through  $F_2$  recovers the  $^1\text{H}$ -decoupled  $^{13}\text{C}$ -nmr spectrum of **I**; projection through  $F_1$  reproduces the  $^1\text{H}$ -nmr spectrum of **I**. Points of intensity in the matrix correlate carbon resonances with their directly attached proton spins.

complete explanation of the purpose of the pulses and delays employed in the execution of this experiment (see Figure 16) is in order. The initial  $90^\circ$  proton pulse tips the proton spin ensemble into the  $x'y'$ -plane where it may precess (evolve) during  $t_1$ , the  $180^\circ$  carbon pulse midway through this period serving to refocus proton-carbon spin couplings. The first fixed delay,  $\Delta_1$ , provides an interval for polarization transfer to develop, the actual transfer produced by the second  $90^\circ$  proton pulse. Optimally,  $\Delta_1$  will be set equal to  $\frac{1}{2}J$  for  $\text{CH}_n$  systems. The  $90^\circ$  carbon pulse serves as the detection pulse for the experiment, the second fixed delay,  $\Delta_2$ , providing a refocusing period for the antiphase CH multiplet components generated by the pulse. The optimal duration of a CH system is  $\frac{1}{2}J$  although a period of  $\frac{1}{4}J$  provides a compromise for systems containing  $\text{CH}_n$  systems where  $n = 1, 2$  and  $3$ . Finally, at the end of the second fixed delay, the proton decoupler is gated back on and the carbon FID recorded. By variation of the duration of  $t_1$ , carbon resonances are amplitude modulated by proton chemical shifts of the directly attached protons (as offset from the  $^1\text{H}$ -transmitter). To provide the equivalent of quadrature detection in both frequency dimensions,  $F_1$  and  $F_2$ , phase cycling is employed, the principles of which have been thoroughly discussed by Freeman and co-workers [58,59].

To complete the assignment of the protonated carbon resonances of **I**, it is convenient to utilize the proton assignments garnered from the COSY spectrum or alternatively, assignments made from the carbon spectrum on the

basis of spin-coupling constants or spin-lattice relaxation times. Thus, we may begin the assignment of the protonated carbon resonances with the ABMX spin system from the COSY spectrum shown in Figure 11. Thus, the H9 resonance, which was assigned to the doublet resonating at  $\delta = 8.72$  [60] is seen to correlate with the carbon resonance at  $\delta = 122.94$  (Figure 18). Assignments for the remaining H6, H7 and H8 resonances (see Table I and Figure 12) follow straight-forwardly from the proton resonance assignments made through the COSY experiment (Table II). Interestingly, it should be noted that the C8 resonance, which is assigned to the signal observed at  $\delta = 126.04$  cor-

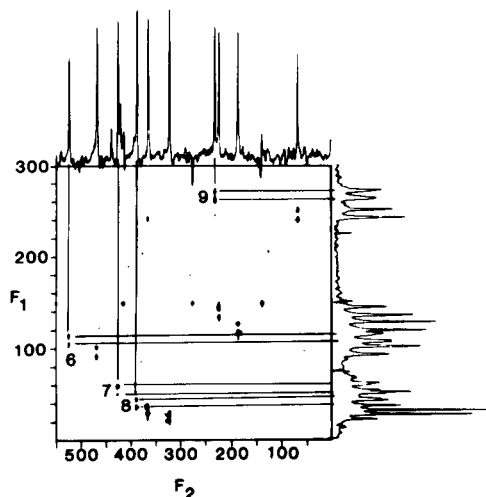


Figure 18. Contour plot of the two-dimensional proton-carbon chemical shift correlation experiment showing the carbon resonances correlated with the protons of the ABMX spin system comprised of H6, H7, H8 and H9.

responds to the second of the carbons exhibiting a shorter spin-lattice relaxation time thus establishing the axis of anisotropic reorientation through both ends of the molecular framework. In principle, this information could be utilized to complete the assignment on the basis of differences in relaxation times as has been done in the case of analogs of the phenarsazine chloride system [50,53] according to the method of Platzner [90]. However, with the availability of the COSY and proton-carbon chemical shift correlation data, the necessity for performing the somewhat tedious and complex calculations necessary to establish the exact orientation of the axis and all of the proton-carbon bond vectors is obviated. Furthermore, the possibility of misassignments because of relatively small differences between relaxation times is eliminated, the proton-carbon chemical shift correlation experiment providing unequivocal assignments.

Assignments for the carbons attached to the protons of two of the remaining three spin systems was accomplished

in a fashion analogous to that just detailed for the ABMX spin system. Thus, the two pairs of proton resonances assigned to H10 and H11 are correlated with the carbons resonating at  $\delta = 119.67$  and  $122.02$  respectively as shown in Figure 19. Similarly, the assignments of the C4

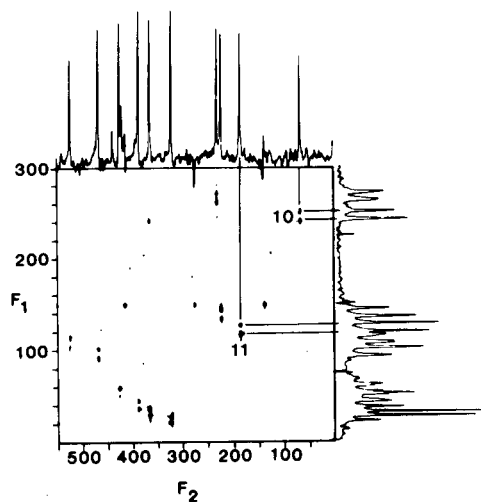


Figure 19. Contour plot of the two-dimensional proton-carbon chemical shift correlation experiment showing the carbon resonances correlated with the protons of the AX spin system comprised of H10 and H11.

and C5 resonances to the signals observed at  $\delta = 122.76$  and  $127.63$  follows from the proton assignments of the corresponding H4/H5 AB spin system as shown in Figure 20.

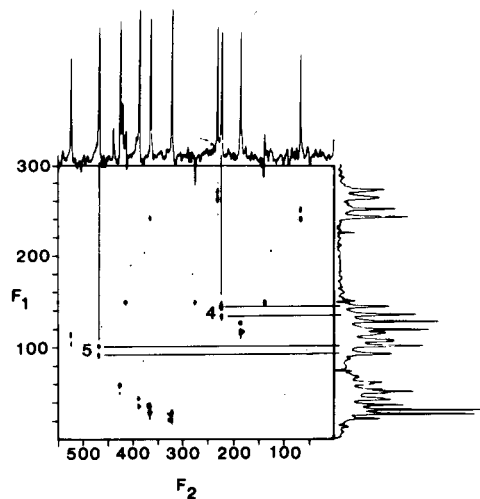


Figure 20. Contour plot of the two-dimensional proton-carbon chemical shift correlation experiment showing the carbon resonances correlated with the proton spins of the AB spin system comprised of H4 and H5.

M. Iwao, M. L. Lee and R. N. Castle

Completion of the assignment of the protonated carbon resonances finally requires the assignment of the H1/H2 AB spin system or alternatively the assignment of one of the carbon resonances through some independent parameter which can in turn be used to assign the proton resonances. In this case, since the C2 resonance has been assigned on the complementary bases of the  $^1\text{H}$ - $^{13}\text{C}$  spin-coupling constant and the spin-lattice ( $T_1$ ) relaxation times, we may thus employ the proton-carbon chemical shift correlation experiment in a sense which is the reverse of that in the preceding assignments. Thus, the C2 resonance which is assignable to the signal observed at  $\delta = 125.59$  correlates with the proton resonance observed at  $\delta = 7.55$  (Figure 21), thereby allowing the assignment of the final remaining proton resonance at  $\delta = 7.51$  to H1 with the assignment of the correlated carbon resonance at  $\delta = 124.75$  to C1.

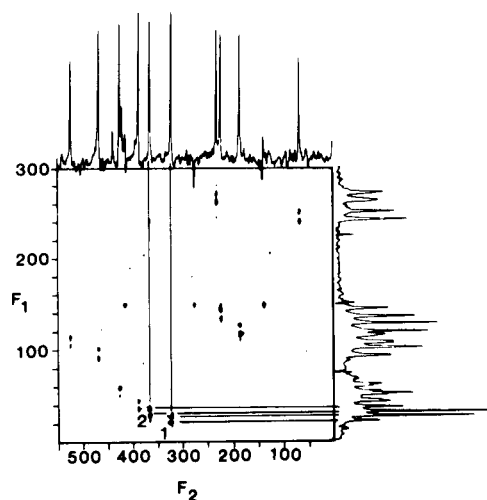


Figure 21. Contour plot of the two-dimensional proton-carbon chemical shift correlation experiment showing the carbon resonances correlated with the AB spin system comprised of H1 and H2. Unlike the other spin systems in the molecule, the C2 resonance was first assigned on the basis of its one-bond heteronuclear spin-coupling constant. Given this assignment, the proton resonance at  $\delta = 7.55$  was assigned as H2 thereby permitting the assignment of the remaining proton resonance at  $\delta = 7.51$  as H1, the correlated carbon at  $\delta = 124.79$  clearly assignable as C1.

#### Assignment of the Quaternary Carbon Resonances.

Assigning the quaternary carbon resonances presents a somewhat different and more formidable problem than that associated with the assignment of the protonated carbon resonances. Unfortunately, the quaternary carbon resonances cannot be assigned on the basis of chemical

shift arguments with any degree of certainty for the same reasons as in the case of their protonated counterparts. While somewhat more soundly based assignments could presumably be made on the basis of heteronuclear spin-coupling constants, these are also potentially equivocal, leaving the assignment of these resonances through the application of two-dimensional double quantum coherence carbon nmr as the sole unequivocal means of making these assignments.

Table IV

Assignments of the protonated carbon resonances of phenanthro[1,2-*b*]thiophene (**I**) derived from the proton-carbon chemical shift correlation experiment.

Position	$\delta$ $^{13}\text{C}$		$\Delta\delta$	$\delta$ $^1\text{H}$
	observed	calcd.		
1	124.74	124.0	+0.7	7.51
2	125.59	126.4	-0.8	7.55
4	122.76	126.9	-4.1	8.09
5	127.63	126.9	+0.7	7.87
6	128.74	128.5	+0.2	7.94
7	126.78	126.5	+0.3	7.66
8	126.03	126.5	-0.5	7.62
9	122.94	122.6	+0.3	8.72
10	119.67	118.3	+1.4	8.61
11	122.02	121.7	+0.3	8.00

Two-dimensional double quantum coherence carbon nmr spectroscopy, like its one-dimensional counterpart the INADEQUATE experiment [91], allows the direct examination of natural abundance carbon-carbon spin-coupling. Since only about 1 molecule in every 10,000 contains adjacent  $^{13}\text{C}$ -nuclides, there is obviously an enormous dynamic range difference in the signal intensities from the carbon-carbon spin-coupled resonances and their isolated  $^{13}\text{C}$  counterparts. To overcome these differences, extensive phase cycling of the experiment is employed to effectively "cancel" the signals from the unwanted, isolated  $^{13}\text{C}$  spins [91,92]. In this manner, we may directly examine the carbon-carbon coupled spectrum, making assignments through the double quantum frequencies which are the algebraic sum of the offsets of the coupled carbon resonances from the transmitter as has been described by Freeman and co-workers [93,94] and recently applied to several practical problems [95-101].

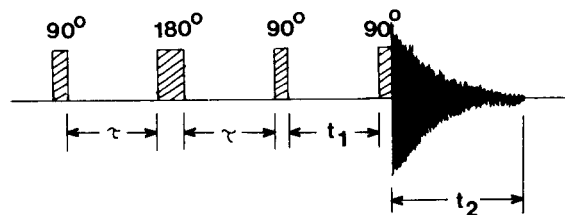


Figure 22. Pulse sequence schematic for the two-dimensional double quantum coherence  $^{13}\text{C}$ -nmr experiment.

The pulse sequence for the two-dimensional double quantum coherence experiment is shown in Figure 22. To circumvent the longer relaxation times of the quaternary carbons of **1**, the sample was doped with Cr(acac)<sub>3</sub>. Despite

Figure 22

this measure, signal-to-noise ratios for the quaternary carbon resonances in the experiment were still rather poor thus preventing the assignment of all of the quaternary carbons by this means. Nevertheless, it was possible to tentatively assign the C3a, C9a and C11a resonances despite the poor signal-to-noise ratios, these assignments shown in Table V, differing significantly from those which would be made on the basis of chemical shift calculation arguments. Assignments for the remaining quaternary carbon resonances must thus still be regarded as potentially equivocal. Further work to complete this final phase of the assignment of **1** is still underway and upon completion, will be correlated with the observed long range heteronuclear spin-coupling constants in an effort to establish a more convenient means of assigning these carbons in eventual spectral examinations of analogs of this system. Results of these efforts will be forthcoming.

Table V

Calculated and observed <sup>13</sup>C-nmr chemical shifts of the quaternary carbons of phenanthro[1,2-*b*]thiophene.

Position	$\delta$ <sup>13</sup> C		$\Delta\delta$
	observed	calcd.	
3a	137.83 [a]	139.8	-2.0
3b	127.08	126.1	+1.0
5a	131.67 [a]	132.0	-0.3
9a	127.08 [a]	130.3	-3.2
9b	130.73	126.1	+4.6
11a	138.83 [a]	137.7	+1.1

[a] Resonances assigned from <sup>13</sup>C-<sup>13</sup>C double quantum two-dimensional nmr experiment. Assignments of the remaining resonances may be permutable as these resonances were not visible with the signal-to-noise levels available in the experiment.

### Summary of the Assignment of Complex Spectra Through the Concerted Application of Two-Dimensional NMR Experiments.

The assignment of the proton and carbon nmr spectra of phenanthro[1,2-*b*]thiophene (**1**), although not a large molecule, represents a substantial challenge to the spectroscopist because of the considerable overlap of resonances in the proton spectrum and the proximity of the resonances in the carbon spectrum. By combining two-dimensional nmr experiments, however, the assignment of these spectra is made considerably more straight-forward. Of the techniques utilized in this study, it seems clear that the COSY and proton-carbon chemical shift correlation experiments will hold the most promise for systems such as the polynuclear aromatics and heteroaromatics. These experi-

ments, particularly when supplemented by other experiments whether conventional or two-dimensional, may be expected to lead to assignments which would have been impossible only a few years ago. It is our expectation that spectroscopists equipped with a working knowledge of these techniques and those presently under development in other laboratories will report the successful structural investigation of increasingly more complex molecules.

### EXPERIMENTAL

Instrument parameters utilized in the acquisition of the spectra described in this work will be presented in detail to enable comparisons between the experiments. With the exception of the T<sub>1</sub> relaxation time measurements, all other spectra were acquired on a Varian XL-200 spectrometer operating at frequencies of 200.057 and 50.039 for <sup>1</sup>H and <sup>13</sup>C respectively. The spin-lattice (T<sub>1</sub>) relaxation times were measured on a Varian XL-100-15 spectrometer equipped with a Nicolet 1180 data system interfaced through a NIC Model 293A' pulse programmer. The spin-lattice relaxation times were measured using the inversion-recovery pulse sequence with a total of fifteen evolution delays. To minimize changes in homogeneity during the course of the experiment, the evolution values were repetitively cycled. Computed relaxation times were obtained using the Three-Parameter Fitting Program of Kowalewski and co-workers [54] and are assumed to be accurate to the level of  $\pm 5\%$ . All spectra were taken on a 2.15M sample of **1** dissolved in deuteriochloroform.

The conventional <sup>1</sup>H-nmr spectrum of **1** was acquired using a total sweep width of 2600 Hz digitized with 15,600 data points with a flip angle of 56°. No digital filtering of the data was done. Total acquisition time for the proton nmr spectrum was 12 seconds (Figure 1).

The conventional <sup>13</sup>C-nmr spectrum of **1** was collected using a sweep width of 15 KHz digitized with 32K data points with a 90° pulse and an acquisition time of 10.667 seconds. A total of 176 accumulations were taken. The initial free induction decay (FID) was smoothed with a Lorentzian weighting function of 0.159 and an apodization factor of 2.0. Total spectral acquisition time was 0.73 hour (Figure 2).

The auto-correlated two-dimensional <sup>1</sup>H-nmr spectrum was obtained using an initial time domain (S(t<sub>1</sub>,t<sub>2</sub>)) consisting of 1024 × 256 points for t<sub>2</sub> and t<sub>1</sub> respectively. Each increment of t<sub>1</sub> was scanned 12 times. The spectral window in both dimensions was 300 Hz giving an acquisition time of 1.708 seconds. Both dimensions were digitally filtered with a positive exponential of 0.7 and an apodization factor of 0.45. Total performance time for the experiment was 1.5 hours (see Figures 10-14).

The heteronuclear two-dimensional J-resolved (2DJ) spectrum was also acquired using an initial data matrix consisting of 1024 × 256 points for t<sub>2</sub> and t<sub>1</sub> respectively. A spectral width of 1200 Hz was used in the F<sub>2</sub> frequency (chemical shift) dimension and 250 Hz in the F<sub>1</sub> frequency dimension (J dimension). An acquisition time of 0.427 seconds and a delay of 0.973 seconds were used giving a cycle time of 1.4 seconds. A total of 148 transients was accumulated for each of the 256 increments of t<sub>1</sub>. The time domain data were multiplied in each dimension by an exponential sensitivity factor with a constant of 0.159 and an apodization factor of 2.0. Total performance time for the experiment was 14.7 hours.

Two-dimensional proton-carbon chemical shift correlation was performed using an initial S(t<sub>1</sub>,t<sub>2</sub>) data matrix which consisted of 1024 × 150 points. The interferograms in the t<sub>1</sub> dimension were zero filled to 512 points before Fourier transformation with respect to t<sub>1</sub>. An acquisition time of 0.931 seconds and a delay of 9.0 seconds was used. The  $\Delta_1$  and  $\Delta_2$  values calculated for a <sup>1</sup>J<sub>CH</sub> of 160 Hz, were 3.12 × 10<sup>-3</sup> and 2.08 × 10<sup>-3</sup> seconds respectively. Total acquisition time for the experiments was 39.7 hours (over weekend).

The two-dimensional carbon-carbon double quantum coherence experiment was accumulated using 15,808 transients on each of 64 increments. A spectral window of 1200 Hz was used in both dimensions. Additionally, no delay was employed since the sample was doped with

Cr(acac)<sub>3</sub> to shorten the longitudinal relaxation times. An acquisition time of 0.427 seconds was used (1024 data points) in the  $t_2$  dimension. A  $J_{CC} = 65$  Hz gave a calculated delay of  $3.84 \times 10^{-3}$  seconds. Total accumulation time for the experiment was 120 hours. Despite the precautions in doping the sample to reduce the relaxation times and the relatively large number of acquisitions used per point in the second dimension, three of the quaternary carbon resonances failed to give adequate signal-to-noise thus leaving these three resonances as potentially permutable assignments. Assignments for the other resonances obtained through this experiment confirmed those made through the other two-dimensional experiments described above.

#### Acknowledgements.

The authors of this work are indebted to several foundations and agencies for the funding which they have provided. In particular, G. E. M. and M. R. W., III would like to acknowledge the generous support of the Robert A. Welch Foundation through Grants No. E-792 and E-183 respectively. We also acknowledge the support of the National Science Foundation in the form of Grant No. CHE75-06162 which provided the funds for the XL-100 spectrometer system at the University of Houston which was used for a portion of this work. Finally, we would also like to express our appreciation of the support of the Department of Energy through contract No. DE-AC02-79EV10237 to R. N. C. and M. L. L. which provided the phenanthro[1,2-*b*]thiophene employed in this study and of Mrs. Cathy Meier for the preparation of this manuscript.

#### REFERENCES AND NOTES

- [1] To whom inquiries should be addressed. Presented, in part, at the 184th National Meeting of the American Chemical Society, Kansas City, MO, Sept 12-17, 1982, Abstract MEDI 67.
- [2] A. Dipple, in "Chemical Carcinogens", C. E. Searle, ed, ACS, Monograph 173, American Chemical Society, Washington, DC, 1976, p 245.
- [3] M. L. Lee, M. V. Novotny and K. D. Bartle, "Analytical Chemistry of Polycyclic Aromatic Compounds", Academic Press, New York, NY, 1981.
- [4] M. L. Lee, C. Willey, R. N. Castle and C. M. White, in "Polynuclear Aromatic Hydrocarbons: Chemistry and Biological Effects", A. Bjorseth and A. J. Dennis, eds, Battelle Press, Columbus, Ohio, 1980, pp 59-73.
- [5] C. M. White and M. L. Lee, *Geochim. Cosmochim. Acta*, **44**, 1825 (1980).
- [6] C. Willey, M. Iwao, R. N. Castle and M. L. Lee, *Anal. Chem.*, **53**, 400 (1981).
- [7] R. C. Kong, M. L. Lee, Y. Tominaga, R. Pratap, M. Iwao, R. N. Castle and S. A. Wise, *J. Chromatogr. Sci.*, **20**, 502 (1982).
- [8] Y. Tominaga, R. N. Castle and M. L. Lee, *J. Heterocyclic Chem.*, **19**, 1125 (1982).
- [9] Y. Tominaga, R. Pratap, R. N. Castle and M. L. Lee, *ibid.*, **19**, 859 (1982).
- [10] R. Pratap, Y. Tominaga, R. N. Castle and M. L. Lee, *ibid.*, **19**, 865 (1982).
- [11] Y. Tominaga, R. Pratap, R. N. Castle and M. L. Lee, *ibid.*, **19**, 871 (1982).
- [12] R. Pratap, R. N. Castle and M. L. Lee, *ibid.*, **19**, 439 (1982).
- [13] R. Pratap, M. L. Lee and R. N. Castle, *ibid.*, **19**, 219 (1982).
- [14] R. Pratap, M. L. Lee and R. N. Castle, *ibid.*, **18**, 1457 (1981).
- [15] Y. Tominaga, M. L. Lee and R. N. Castle, *ibid.*, **18**, 967 (1981).
- [16] R. Pratap, Y. Tominaga, M. L. Lee and R. N. Castle, *ibid.*, **18**, 973 (1981).
- [17] Y. Tominaga, M. L. Lee and R. N. Castle, *ibid.*, **18**, 977 (1981).
- [18] R. D. Thompson, M. Iwao, M. L. Lee and R. N. Castle, *ibid.*, **18**, 981 (1981).
- [19] M. Iwao, M. L. Lee and R. N. Castle, *ibid.*, **17**, 1259 (1980).
- [20] G. E. Maciel and M. J. Sullivan "13C-NMR Characterization of Solid Fossil Fuels Using Cross-Polarization and Magic Angle Spinning", Chapter in "NMR Spectroscopy: New Methods and Applications", G. C. Levy, ed, American Chemical Society, Symposium Series Vol 191, Washington, DC, 1982, pp 318-343 and references contained therein.
- [21] R. S. Ozbuko, G. W. Buchanon and I. C. P. Smith, *Can. J. Chem.*, **52**, 2493 (1974).
- [22] W. Kitching, M. Bullpitt, D. Gartshore, W. Adcock, T. C. Khou, D. Doddrell and I. D. Rae, *J. Org. Chem.*, **42**, 2411 (1977).
- [23] W. Anderson, R. Freeman and H. Hill, *Pure Appl. Chem.*, **32**, 27 (1972).
- [24] I. Morishima, K. Kawakami, T. Yonezawa, K. Gato and M. Imanari, *J. Am. Chem. Soc.*, **94**, 6555 (1972).
- [25] R. E. Wasylshen, B. E. Pettit and W. Danchura, *Can. J. Chem.*, **55**, 3602 (1977).
- [26] V. G. Berechnoi and N. M. Sugeev, *Zh. Strukt. Khim.*, **16**, 136 (1975).
- [27] F. W. Wehrli, "Organic Structure Assignments Using 13C Spin-Relaxation Data", in "Topics in Carbon 13 NMR Spectroscopy", G. C. Levy, ed, Vol 2, Wiley-Interscience, NY, 1976, pp 343-391.
- [28] P. C. Lauterbar, *J. Am. Chem. Soc.*, **83**, 1838 (1961).
- [29] D. Lauer, E. L. Motell, D. Traficante and G. E. Maciel, *ibid.*, **94**, 5335 (1972).
- [30] R. H. Martin, J. Moriau and N. Defay, *Tetrahedron*, **30**, 179 (1974).
- [31] W. Kitching, M. Bullpitt, D. Doddrell and W. Adcock, *Org. Magn. Reson.*, **6**, 289 (1974).
- [32] R. J. Highet and J. M. Edwards, *J. Magn. Reson.*, **17**, 336 (1975).
- [33] J. Seita, T. Drakenberg and J. Sandström, *Org. Magn. Reson.*, **11**, 239 (1978).
- [34] R. A. Bell, C. L. Chan and B. G. Sayer, *J. Chem. Soc., Chem. Commun.*, 67 (1972).
- [35] N. K. Wilson and J. B. Stothers, *J. Magn. Reson.*, **15**, 31 (1974).
- [36] M. L. Caspar, J. B. Stothers and N. K. Wilson, *Can. J. Chem.*, **53**, 1958 (1975).
- [37] L. Ernst, *J. Magn. Reson.*, **22**, 279 (1976).
- [38] S. Braun and J. Kinkeldei, *Tetrahedron*, **33**, 1827 (1977).
- [39] P. E. Hansen, *Org. Magn. Reson.*, **12**, 109 (1979) and references contained therein.
- [40] W. P. Aue, E. Bartholdi and R. R. Ernst, *J. Chem. Phys.*, **64**, 2229 (1976).
- [41] A. Bax, R. Freeman and G. Morris, *J. Magn. Reson.*, **42**, 164 (1981).
- [42] Care should be taken to note that  $t_1$  and  $t_2$ , the two time variables in two-dimensional nmr spectroscopy, have no relationship to the spin-lattice relaxation time,  $T_1$ , or the spin-spin relaxation time,  $T_2$ .
- [43] G. Bodenhausen, R. Freeman, R. Niedermeyer and D. L. Turner, *J. Magn. Reson.*, **26**, 133 (1977).
- [44] R. L. Vold, J. S. Waugh, M. P. Klein and D. E. Phelps, *J. Chem. Phys.*, **48**, 3831 (1968).
- [45] R. Freeman and H. D. W. Hill, *ibid.*, **51**, 3140 (1969).
- [46] R. R. Ernst, W. P. Aue, P. Bachmann, A. Hohener, M. Linder, B. Meier, L. Müller, A. Wokaun, K. Nagayama, K. Wuthrich and J. Jeener, "Application of Two Dimensional Spectroscopy to Problems of Physical, Chemical and Biological Relevance", "Magnetic Resonance and Related Phenomena", Proceedings XXth Congress Ampere, Tallin, Estonia, E. Kundla, E. Lippmaa and T. Saluvere, eds, Springer-Verlag, NY, 1979, pp 15-18.
- [47] Interferograms are analogous to free induction decays in the information that they contain. We will exclusively employ the term interferogram to refer to time domain information of the type  $S(F_2, t_1)$ .
- [48] P. Geneste, J.-L. Olive, S. N. Ung, M. El Amoudi El Faghi, J. W. Easton, H. Bierbeck and J. K. Saunders, *J. Org. Chem.*, **44**, 2887 (1979).
- [49] R. T. Gampe, Jr., G. E. Martin, A. C. Pinto and R. A. Hollins, *J. Heterocyclic Chem.*, **18**, 155 (1981).

- [50] M. Jay and G. E. Martin, *ibid.*, **19**, 241 (1982).
- [51] S. Puig-Torres, G. E. Martin, J. J. Ford, M. R. Willcott, III and K. Smith, *ibid.*, **19**, 1441 (1982).
- [52] C. H. Womack, R. T. Gampe, Jr., B. K. Lemke, K. N. Sawhney, T. L. Lemke and G. E. Martin, *ibid.*, **19**, 1105 (1982).
- [53] M. Jay and G. E. Martin, *ibid.*, **20**, 527 (1983).
- [54] J. G. Kowalewski, G. C. Levy, L. F. Johnson and L. Palmer, *J. Magn. Reson.*, **26**, 553 (1977).
- [55] F. J. Weigert and J. D. Roberts, *J. Am. Chem. Soc.*, **90**, 3543 (1968).
- [56] J. Jeener, abstract of a paper presented at an Ampere International Summer School, Basko Polje, Yugoslavia, 1971.
- [57] A. Bax and R. Freeman, *J. Magn. Reson.*, **44**, 542 (1981).
- [58] G. Bodenhausen, R. Freeman and D. L. Turner, *ibid.*, **27**, 511 (1977).
- [59] G. Bodenhausen, R. Freeman, G. A. Morris, R. Niedermeyer and D. L. Turner, *ibid.*, **25**, 559 (1977).
- [60] P. M. G. Bavin, K. D. Bartle and J. A. S. Smith, *Tetrahedron*, **21**, 1087 (1965); B. P. Dailey, *J. Chem. Phys.*, **36**, 2443 (1962); R. H. Martin, N. Defay, F. Greeto-Evrard and S. Delavarene, *Tetrahedron*, **20**, 1073 (1964).
- [61] L. Müller, A. Kumar and R. R. Ernst, *J. Chem. Phys.*, **63**, 5490 (1976).
- [62] G. Bodenhausen, R. Freeman and D. L. Turner, *ibid.*, **65**, 839 (1976).
- [63] L. Müller, A. Kumar and R. R. Ernst, *J. Magn. Reson.*, **25**, 383 (1977).
- [64] D. M. Thomas, M. R. Bendall, D. T. Pegg, D. M. Dodrell and J. Field, *ibid.*, **42**, 298 (1981).
- [65] G. Bodenhausen, R. Freeman and G. A. Morris, *ibid.*, **23**, 171 (1976).
- [66] G. A. Morris and R. Freeman, *ibid.*, **29**, 433 (1978).
- [67] R. Freeman, G. A. Morris and J. T. Robinson, *J. Chem. Soc., Chem. Commun.*, 754 (1976).
- [68] G. E. Martin, *J. Heterocyclic Chem.*, **15**, 1539 (1978).
- [69] J. C. Turley and G. E. Martin, *Spectros. Letters*, **11**, 681 (1978).
- [70] O. M. Sejiny and G. E. Martin, *J. Heterocyclic Chem.*, **17**, 1741 (1980).
- [71] S. R. Caldwell, G. E. Martin, S. H. Simonsen, R. R. Inners and M. R. Willcott, III, *ibid.*, **18**, 479 (1981).
- [72] G. E. Martin, J. C. Turley and L. Williams, *ibid.*, **14**, 1249 (1977).
- [73] G. E. Martin, *ibid.*, **17**, 429 (1980).
- [74] S. R. Caldwell, J. C. Turley and G. E. Martin, *ibid.*, **17**, 1153 (1980).
- [75] S. R. Caldwell and G. E. Martin, *ibid.*, **17**, 989 (1980).
- [76] R. L. Vold and S. O. Chan, *J. Chem. Phys.*, **53**, 449 (1970).
- [77] R. Freeman and H. D. W. Hill, *ibid.*, **54**, 301 (1971).
- [78] G. Bodenhausen, R. Freeman, R. Niedermeyer and D. L. Turner, *J. Magn. Reson.*, **24**, 291 (1976).
- [79] A. A. Maudsley and R. R. Ernst, *Chem. Phys. Letters.*, **50**, 368 (1977).
- [80] G. Bodenhausen and R. Freeman, *J. Magn. Reson.*, **28**, 471 (1977).
- [81] R. Freeman and G. A. Morris, *J. Chem. Soc., Chem. Commun.*, 684 (1978).
- [82] G. Bodenhausen and R. Freeman, *J. Am. Chem. Soc.*, **100**, 320 (1978).
- [83] M. R. Bendall, D. T. Pegg, D. M. Dodrell and J. Field, *ibid.*, **103**, 934 (1981).
- [84] G. A. Morris and L. D. Hall, *ibid.*, **103**, 4703 (1981).
- [85] A. Bax and G. A. Morris, *J. Magn. Reson.*, **42**, 501 (1981).
- [86] G. A. Morris, *ibid.*, **44**, 277 (1981).
- [87] M. R. Bendall, D. T. Pegg, D. M. Dodrell and D. M. Thomas, *ibid.*, **46**, 43 (1982).
- [88] M. J. Musmar, A. J. Weinheimer, M. Alam, G. E. Martin, R. R. Inners, M. R. Willcott, III and R. E. Hurd, *J. Am. Chem. Soc.*, in press.
- [89] T.-M. Chan and J. L. Markley, *ibid.*, **104**, 4010 (1982).
- [90] N. Platzner, *Org. Magn. Reson.*, **11**, 350 (1978).
- [91] A. Bax, R. Freeman and S. P. Kempell, *J. Am. Chem. Soc.*, **102**, 4849 (1980).
- [92] A. Bax, R. Freeman and S. P. Kempell, *J. Magn. Reson.*, **41**, 349 (1980).
- [93] A. Bax, R. Freeman and T. A. Frenkiel, *J. Am. Chem. Soc.*, **103**, 2102 (1981).
- [94] A. Bax, R. Freeman, T. A. Frenkiel and M. H. Levitt, *J. Magn. Reson.*, **43**, 478 (1981).
- [95] R. Richarz, W. Ammann and T. Wirthlin, *ibid.*, **45**, 270 (1981).
- [96] A. Neszmelyi and G. Lukacs, *J. Chem. Soc., Chem. Commun.*, 999 (1981).
- [97] D. L. Turner, *Mol. Phys.*, **44**, 1051 (1981).
- [98] J. A. Robinson and D. L. Turner, *J. Chem. Soc., Chem. Commun.*, 148 (1982).
- [99] A. C. Pinto, M. L. A. Goncalves, R. B. Filho, A. Neszmelyi and G. Lukacs, *ibid.*, 293 (1982).
- [100] T. H. Mareci and R. Freeman, *J. Magn. Reson.*, **48**, 158 (1982).
- [101] R. Freeman, T. Frenkiel and M. B. Rubin, *J. Am. Chem. Soc.*, **104**, 5545 (1982).